INTERNATIONAL JOURNAL
FOR RESEARCH

IN APPLIED SCIENCE & ENGINEERING TECHNOLOGY

Multi-GNSS Software Receiver Design Optimization for Accuracy Improvement

Jasmien Hassanien[1], Alaa Elrouby[2]

[1]MSc student, [2]Profesor, Electrical and Electronic Engineering Department, Ankara Yildirim Beyazit University

Abstract: Recently, tremendous research has been conducted on Global navigation satellite systems (GNSS) software receivers to better serve the current challenging environments that suffers from multipath fading. Therefore, the development of GNSS receivers has seen a new rush toward a multi-GNSS as a solution for fading problems. In this paper, a multi-GNSS software receiver is designed, optimized, and its performance is presented. The implemented software receiver covers three different signals from two GNSS constellations, namely GPS L1, GPS L2, and Galileo E1. In this paper. the fundamentals of stages of GNSS signal reception (acquisition, tracking, and navigation) are discussed where each stage is customized and optimized for each considered signal and the stage of mutli-GNSS data combination is optimized afterword. The performance of the optimized multi-GNSS software receiver is examined under different combination scenarios where the Least-Square Estimation (LSE) method using precise positioning (PP) algorithms is adopted. Results showed that using multi-GNSS receiver enhances the accuracy of Position, Velocity, and Timing (PVT) solution.
Keywords: GNSS, PVT, GPS, Galileo, and accuracy.

I. INTRODUCTION

Recently, the function of Global Navigation Satellite Systems (GNSS) has been considered an essential part of our daily life. For years the Global Positioning System (GPS), which was developed by the United States in the 1970s, was the most popular navigation system. Thereafter, the Russian Global Orbiting Navigation Satellite System (GLONASS) re-established Full Operational Capability (FOC) by late 2011. Besides those two GNSS which are already in full service, two new systems were added, the European (Galileo) and the Chinese (BeiDou), both of which are currently under development and are expected to reach FOC in the coming years. As a result, today we have four independent GNSS constellations that are fully or partially operational. However, challenging environments such as urban areas have recently become a concern for many civilian and military systems as it negatively affects positioning accuracy because of satellite blockage by buildings as well as multipathing. Accordingly, the optimization of GNSS receivers has recently been a serious topic for research and many studies have been conducted to enhance the accuracy and performance of GNSS receivers under harsh signal conditions. Multi-GNSS receivers are considered one of the main solutions to overcome the above-mentioned challenges. Multi-GNSS receivers utilize signals from multi constellations and/or different frequency bands [1] which helps in 1) increasing the number of visible satellites which improves navigation signals availability, and 2) selecting the strongest signals among available ones. Consequentially, accuracy, and reliability enhancement are driven. In this paper, a multi-GNSS software receiver based on GPS-L1, GPS-L2, and Galileo-E1 signals is designed, optimized, and implemented with focus on positioning accuracy improvement. First, the implemented design of the multi-GNSS software receiver is discussed in section II, where a brief description of the main stages of the receiver is presented. Those stages are acquisition, tracking, and navigation solutions. The optimization of multi-GNSS receiver is performed in two steps: 1) optimizing each stage of the GNSS receiver for each individual constellation/signal, 2) optimize the combination of solutions from the different signals of the multi-GNSS receiver. For combination of solutions from different GNSS signals, the Least-Square Estimation (LSE) using precise positioning (PP) algorithms [2] is adopted and optimized. The details of design optimization as well as the experimental results for date combination which are examined under four different scenarios -based on all different combinations of considered signals (L1, E1 and L2- are presented in section III while the conclusions are presented in section IV.

II. DESIGN AND IMPLEMENTATION OF THE MULTI-GNSS SOFTWARE RECEIVER

As previously mentioned, our aim is to enhance the positioning accuracy by using multi-GNSS solution. In this section, the optimized design of the multi-GNSS receiver is presented, and the main software stages will be briefly discussed. The advantage of using multi-GNSS for reliability and accuracy had been reported in literature. [3] for example had reported that by combining L2C, with L1 C/A, enhanced reliability, and greater operating range will be achieved. L2C and Galileo signals are using the forward error correction (FEC) technique that protects the data components by allowing the receiver to detect and correct the errors caused by noise[4].

Consequently, GPS-L1, GPS-L2, and Galileo-E1 signals were chosen to be used in this study with the possibility of using the same approach and receiver structure to consider more signals in the future. The chosen signals are from two frequency bands and two different GNSS constellations.

The block diagram and data flow of the software receiver, which is implemented in MATLAB, used in this research is shown in Fig 1. The "SoftGNSS v3.0" open sources, a project of the Danish GPS Center is used as a starting point in this research. The receiver is designed to post-process binary raw data and save the intermediate results from each stage. The details of design optimization of the receiver are presented in the next 7 subsections while for details about the fundamentals of GPS and Galileo, [5] can be consulted.
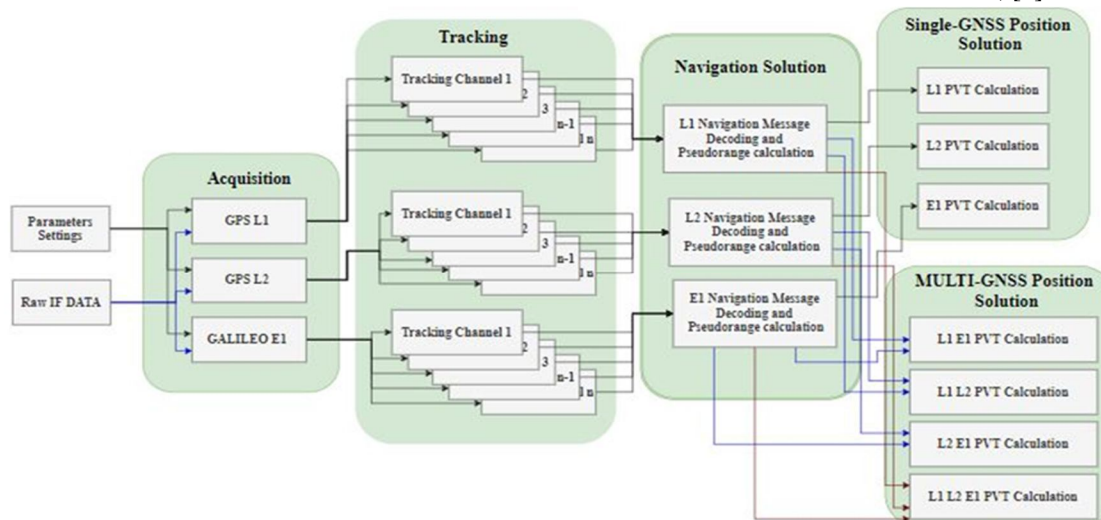

Fig. 1 The Block Diagram and data flow of the implemented software receiver.

A. Signal Acquisition

The acquisition is the first stage in the software receiver where the received signal is correlated with a local replica of satellite pseudo random code (PRN) and the position of the peak is used to estimate the unknown parameters of the incoming signal and find all visible satellites. The unknown parameters are the signal carrier frequency and code delay which is the time delay between the received signal's PRN and the local PRN replica. In general, there are three basic methods for acquisition that differ in complexity and execution time. These methods are Serial Search, Parallel Frequency Space Search, and Parallel Code Phase Search. According to [5], to increase the speed of the acquisition process, parallel acquisition methods are preferred and hence its Implementation based on Fourier transform (FFT) [6] is adopted. This method is the fastest, compared to the others, where the FFT of the generated PRN code must take place only one time for each acquisition. The different modulation techniques for the considered signals have been taken into consideration, for example, GPS signals are using binary phase-shift keying (BPSK) while GALILEO signals are using BOC modulation [7]. Those modulation techniques have different effects in autocorrelation, for example, BPSK signals' autocorrelation has one peak only at zero delays, while in BOC modulation multiple peaks are presented which implies an ambiguity issue. Accordingly, different techniques are implemented in the acquisition stage to fulfil the requirements for each signal to drive a successful acquisition. our results and analysis showed that noisy satellites have negative impact on accuracy. Therefore, noisy satellites are excluded by increasing the acquisition threshold while detecting visible satellites.

B. Signal Tracking

The main purpose of tracking functions is to monitor the changing of the carrier frequency and code delay due to channel conditions variation over time. This stage allows the receiver to wipe the PRN code and the sinusoidal carrier off the received signal. The concept of code/carrier wipes off is that the locally generated code/carrier signal is attempting to be identical to the corresponding incoming signal. By multiplying the locally generated signal and the incoming signal, double intermediate frequency terms are obtained, which can be cancelled by applying a low pass filter. Accordingly, the code and carrier are excluded from the incoming signal leaving us only with the navigation data. Thereafter, by decoding the navigation data, the satellite's navigation message can be extracted, and PVT can be calculated. To achieve this task, the acquisition results are fed into the tracking stage where, the code delay, carrier frequency, and carrier phase are tracked using Delay Lock Loop (DLL), Frequency locked loop (FLL), and Phase Lock Loop (PLL) respectively.

As previously mentioned in the acquisition stage, different signals need different techniques and different settings, therefore, the tracking stage is optimized per each considered signals (L1, E1, & L2) differently. Towards that tracking optimization goals, the order of the used low pass filter and the type of the discriminator utilized. Furthermore, the parameters of the DLL, FLL, and PLL are optimized as well. Further details for different tracking techniques can be found in[5][8][9].

C. Signal Navigation

After decoding navigation messages in the tracking stage from at least four visible satellites and extracting the satellites' information (position, velocity, and time of week (TOW)), the receiver can estimate its position, time, and velocity. This process is performed by comparing the signal transmission time to the receiver time. Then, the pseudo ranges can be calculated by multiplying the speed of light by the signal's travel time. Since the satellite and receiver clock systems are unsynchronized, a clock bias must be taken into consideration. The pseudo range ρ_j relates the position of satellite j and the receiver's position can be written as follows:

$$\rho_j = \sqrt{(x_j - x_r)^2 + (y_j - y_r)^2 + (z_j - z_r)^2} + c \cdot \delta t + \epsilon \quad (1)$$

where (x_j, y_j, z_j), (x_r, y_r, z_r) are the satellite j coordinates and the receiver coordinates, respectively. c refers to the speed of light, δt is the clock bias (the receiver time offset from GNSS system time.), and ϵ includes the contribution of all aggregated errors (due to noise, multipath, ionosphere and troposphere errors). Then, the pseudo ranges from different satellites are combined, and a system of nonlinear equations is formed, with the time bias offset δt, and the position coordinates (x_r, y_r, z_r) as unknowns. That system can be linearized if at least four measurements are available.

D. Single PVT Solution Technique

By linearizing (1) around a nominal state estimate,

$$P_o = [x_o \ y_o \ z_o \ \delta t_o]^T \quad (2)$$

The estimated position and clock bias offset is considered as a vector sum of the approximate estimate P_o, and the difference between the estimated receiver parameters and the linearization point.

$$P = P_o + [\Delta x \ \Delta y \ \Delta z - c \cdot \Delta \delta t]^T \quad (3)$$

By applying Taylor series, the observation equation can be shown in (4), and (5).

$$\rho_j = \rho_{0_j} + \frac{\partial \rho_j}{\partial x_o} \cdot (\Delta x) + \frac{\partial \rho_j}{\partial y_o} \cdot (\Delta y) + \frac{\partial \rho_j}{\partial z_o} \cdot (\Delta z) + c \cdot \Delta \delta t \quad (4)$$

$$\rho_j = \rho_{0_j} - \frac{x_j - x_o}{\rho_{0_j}} \cdot (\Delta x) - \frac{y_j - y_o}{\rho_{0_j}} \cdot (\Delta y) - \frac{z_j - z_o}{\rho_{0_j}} \cdot (\Delta z) + c \cdot \Delta \delta t \quad (5)$$

Where, $\rho_{0_j} = \sqrt{(x_j - x_o)^2 + (y_j - y_o)^2 + (z_j - z_o)^2}$ refers to the predicted pseudo range, and ρ_j is the actual measured pseudo range. From 5,

$$\rho_{0_j} - \rho_j = \frac{x_j - x_o}{\rho_{0_j}} \cdot (\Delta x) + \frac{y_j - y_o}{\rho_{0_j}} \cdot (\Delta y) + \frac{z_j - z_o}{\rho_{0_j}} \cdot (\Delta z) - c \cdot \Delta \delta t \quad (6)$$

Let,

$$\Delta \rho_j = \rho_{0_j} - \rho_j \quad (7)$$

$\Delta \rho$ can be solved by inserting 3 and 7 into 1 to yield the following:

$$\Delta \rho_j = a_{xj} \Delta x + a_{yj} \Delta y + a_{zj} \Delta z - c \cdot \Delta \delta t \quad (8)$$

International Journal for Research in Applied Science & Engineering Technology (IJRASET)
ISSN: 2321-9653; IC Value: 45.98; SJ Impact Factor: 7.429
Volume 9 Issue IX Sep 2021- Available at www.ijraset.com

Where, $a_{xj} = \frac{x_j - x_0}{||s_j - r_j||}$, $a_{yj} = \frac{y_j - y_0}{||s_j - r_j||}$, and $a_{zj} = \frac{z_j - z_0}{||s_j - r_j||}$. s_j denotes the coordinates of the satellite j, and r_j refers to the estimated receiver position. By this method, a system of linear equations is formed in (9).

$$\Delta\rho = H\Delta m \quad (9)$$

Where,

$$\Delta\rho = \begin{bmatrix} \Delta\rho_1 \\ \Delta\rho_2 \\ \Delta\rho_3 \\ \Delta\rho_4 \\ \vdots \\ \Delta\rho_n \end{bmatrix}, H = \begin{bmatrix} a_{x1} & a_{y1} & a_{z1} & 1 \\ a_{x2} & a_{y2} & a_{z2} & 1 \\ a_{x3} & a_{y3} & a_{z3} & 1 \\ a_{x4} & a_{y4} & a_{z4} & 1 \\ \vdots & \vdots & \vdots & \vdots \\ a_{xn} & a_{yn} & a_{zn} & 1 \end{bmatrix}, \text{ and } \Delta m = \begin{bmatrix} \Delta x \\ \Delta y \\ \Delta z \\ -c \cdot \Delta\delta t \end{bmatrix}.$$

H denotes a linear matrix and n is the number of measurements available. This leads to (10), that contains the receiver's position and clock bias.

$$\Delta m = H^{-1}\Delta\rho \quad (10)$$

To estimate user velocity, we used the same technique as position estimation. However, we need to replace (Δx, Δy, Δz, $\Delta\delta t$) by (ΔV_X, ΔV_Y, ΔV_Z, $\Delta F/f_c$) where, (ΔV_X, ΔV_Y, ΔV_Z) donates the time derivative of the estimated user position in the XYZ coordinates, respectively, ΔF represents the Doppler offset due to the relative motion between the satellite and the receiver, and f_c is the carrier frequency of the used GNSS signal. Multiplying $\Delta F/f_c$ and the speed of light, c, gives the clock drift. Thereafter, the observation matrix is the difference between the actual and the measured doppler shift (aka pseudo range rate). Accordingly, the system equation can be written as the following,

$$d = HG \quad (11)$$

Where,

$$d = \begin{bmatrix} \Delta\rho_{r1} \\ \Delta\rho_{r2} \\ \Delta\rho_{r3} \\ \Delta\rho_{r4} \\ \vdots \\ \Delta\rho_{rn} \end{bmatrix}, H = \begin{bmatrix} a_{x1} & a_{y1} & a_{z1} & 1 \\ a_{x2} & a_{y2} & a_{z2} & 1 \\ a_{x3} & a_{y3} & a_{z3} & 1 \\ a_{x4} & a_{y4} & a_{z4} & 1 \\ \vdots & \vdots & \vdots & \vdots \\ a_{xn} & a_{yn} & a_{zn} & 1 \end{bmatrix}, \text{ and } G = \begin{bmatrix} \Delta V_X \\ \Delta V_Y \\ \Delta V_Z \\ -c \cdot \Delta F/f_c \end{bmatrix}.$$

H matrix is the same for both position and velocity, and d is the observation matrix, where,

$$\Delta\rho_r = a_{xj}\Delta V_X + a_{yj}\Delta V_Y + a_{zj}\Delta V_Z - c \cdot \Delta F/f_c$$

From (11), the velocity and the clock drift are estimated as the following,

$$G = H^{-1}d \quad (12)$$

E. Least squares estimation (LSE)

The Least Square Error estimation (LSE) algorithm is utilized to compute the position solution. The previous mentioned process is iterated until the accuracy meets the requirement. From (10) and (12), respectively, the solution by LSE, can be written as follows:

$$\Delta m_{LS} = (H^T H)^{-1} H^T \Delta\rho \quad (13)$$

And for velocity,

$$G_{LS} = (H^T H)^{-1} H^T d \quad (14)$$

Where, $(H^T H)^{-1}$ represents the Dilution of precision (DOP), which is a parameter describes the user/satellite geometry.

F. Multi PVT Solution Mechanization

In Multi-GNSS, each system has a different time reference. Therefore, the PVT combination strategies need to be designed to consider the different clock offsets errors associated with different GNSS systems. Two techniques have been found in the literature which are coarse positioning (CP) and precise positioning (PP). The CP technique is adjusting GPS clock offset as a reference and synchronizing the other GNSS offsets accordingly, here we can conclude that the observation matrix of this technique is the same as the single GNSS observation matrix as we are using only one clock offset, also the minimum number of visible satellites needed for this method is four. However, in the PP technique, the clock offset of each system is calculated separately, where the clock offset for each system used is added in the observation matrix, and the minimum number of the visible satellites is dependent on the number of systems used. By using the PP technique, we already need three visible satellites for the receiver coordinate and one more for the clock offset, accordingly, if we use two GNSS systems we need five visible satellites instead of four, this extra satellite is to accommodate the addition of the clock offset of the second GNSS system as an unknow. We found that the CP methods have a negative effect on accuracy due to the synchronization between different systems. So, in our design, the PP technique is adopted.

G. LSE based on Precise Positioning (PP)

As previously mentioned, in PP technique, an additional unknown parameter appears for each additional GNSS, this unknown refers to the clock offsets of each system used. Therefore, the observation matrix of precise positioning can be written as

$$\Delta\rho_{PP} = H_{PP}\Delta m_{PP} \quad (15)$$

where,

$$\Delta\rho_{PP} = \begin{bmatrix} \rho^1_{GPS,GPST} \\ \vdots \\ \rho^n_{GPS,GPST} \\ \rho^1_{X,XT} \\ \vdots \\ \rho^m_{X,XT} \end{bmatrix}, H_{PP} = \begin{bmatrix} a^1_{x,GPS} & a^1_{y,GPS} & a^1_{z,GPS} & 1 & 0 \\ \vdots & \vdots & \vdots & \vdots & \vdots \\ a^n_{x,GPS} & a^n_{y,GPS} & a^n_{z,GPS} & 1 & 0 \\ a^1_{x,X} & a^1_{y,X} & a^1_{z,X} & 0 & 1 \\ \vdots & \vdots & \vdots & \vdots & \vdots \\ a^m_{x,X} & a^m_{y,X} & a^m_{z,X} & 0 & 1 \end{bmatrix}, \text{and } \Delta m_{PP} = \begin{bmatrix} \Delta x \\ \Delta y \\ \Delta z \\ -c \cdot \Delta\delta t_{GPS} \\ -c \cdot \Delta\delta t_X \end{bmatrix}.$$

The same technique can be used for velocity estimation. The results of this system give the receiver position on the ECEF coordinate system; However, our receiver is implemented to support the conversion to other systems such as ENU and LLH systems. More details about GNSS coordinate systems can be found at [3], n is donating the number of GPS satellites, and m refers to the number of satellites for the GNSS system X. For optimizing the position accuracy in this stage, we designed two modules to minimize the error due to ionosphere and due to troposphere layers, those modules are implemented to calculate the error and subtract it from the measurement.

III. EXPERIMENTAL RESULTS

The different stages of GNSS software receivers mentioned above in section II is implemented in MATLAB code, where we 1) optimized and customized each module (stage) per used signal (namely, L1, E1 & L2), and 2) optimized the data combination stage for better accuracy. To test the performance of the designed and optimized GNSS SW receiver, The data published in [10] is used. These data were recorded from a Spirent GSS8000 RF constellation simulator in a static scenario providing GPS and Galileo signals, With 18 MHz bandwidth and 20MSPS at 4bit I/Q sampling rate.

A. Acquisition Results

By testing different scenarios, the optimum acquisition parameters for each system were provided in Table I.

TABLE I

Optimum acquisition parameter values for L1/L2/E1

Parameters	GPS L1	GPS L2	GAL E1
Frequancy search band (KHz)	14	10	14
Frequancy search bin (Hz)	250	25	500
Acqusiion threshold	4.2	5.55	9
Coherent Integration Time (ms)	11	20	50
Number of visible satellites	6		

Table II indicates the position error comparison of both GPS L1 C/A, GPS L2, and Galileo E1 signals with respect to the effect of the number of visible satellites. We observed that, by excluding weaker signals as shown in Fig.2, the positioning accuracy is enhanced. In other words, reducing the number of noisy visible satellites improves performance in terms of positioning error and coordinate variations. However, by increasing the number of visible satellites we can see that the standard deviation gives a better performance. That contradicting observation requires further analysis of more data.

Table II

Mean and Standard deviation statistics of positioning errors for L1/L2/E1 under different threshold.

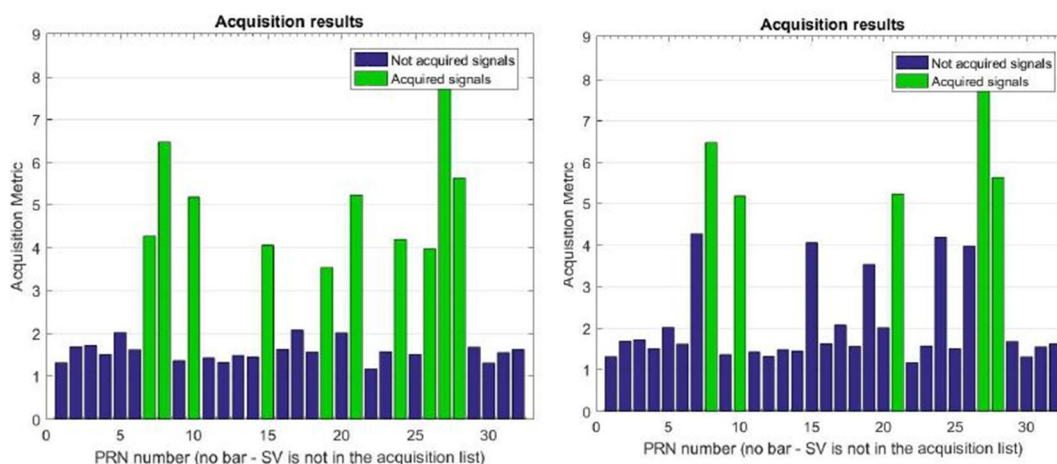| Number of Satellites	Positioning error	GPS L1	GPS L2	GAL E1
5	Mean East (m)	0.7	1.13	0.36
	Mean North (m)	0.04	0.06	0.2
	Mean Up (m)	1.3	1.7	0.9
	Std. East (m)	8.9	26.03	1.35
	Std. North (m)	3.9	9.86	0.59
	Std. Up (m)	7.3	23.5	2.9
10	Mean East (m)	1.6	3.4	0.3
	Mean North (m)	0.3	0.5	0.2
	Mean Up (m)	1.9	3.5	1.5
	Std. East (m)	1.5	5.4	0.7
	Std. North (m)	1.5	5.0	0.3
	Std. Up (m)	2.9	10.1	0.8

Fig. 2 Acquired Satellited of GPS L1 C/A under 2.5 Threshold (Left) and 5 Threshold (Right).

B. *Tracking Results*

To validate the tracking loops and test the positioning performance, 60 seconds of data was used. the Tracking results of GPS L1 C\A are shown in Fig.3, in subplot 1 the I/Q scatter plot shows that the signal energy is mostly contained in the I component, while the Q component is mostly noise, indicating that the PLL is correctly locked. Furthermore, in subplot 4 the magnitude of the prompt correlator is highest compared to early and late correlators, confirming that the DLL tracks the code phase.
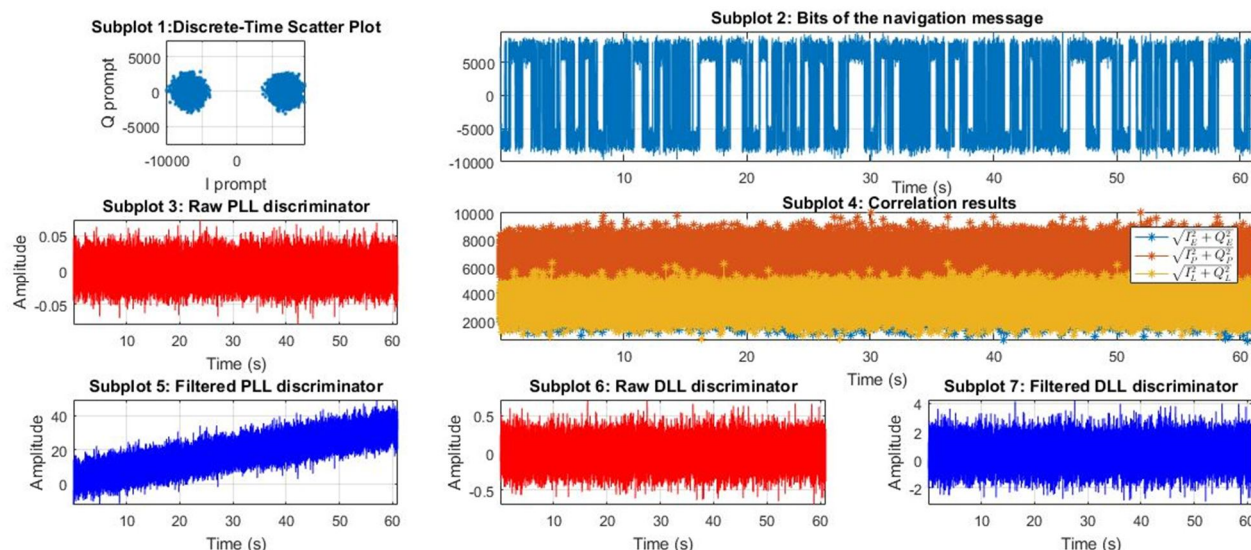

Fig. 3 L1 Tracking Results for PRN 8.

C. *Navigation Solution Results*

To compute the position solution, the Least Square Error estimation (LSE) algorithm is used. In this section, we tested the accuracy of positioning under the effect of different parameters like elevation mask angels and applying the troposphere and ionosphere error corrections. In Table III, the most GNSS system errors are shown.

Table III

GNSS System errors [11].

Contributing Source	Error Range
Satellite clocks	± 2 m
Orbit errors	± 2.5 m
Ionospheric delays	± 5 m
Tropospheric delays	± 0.5 m
Receiver nose	± 0.3 m
Multipath	± 1m

D. *Elevation Mask angels*

One of the parameters influencing positioning accuracy is the satellite elevation mask angle (aka elevation cut-off), which is the minimum elevation angle reflecting signal shielding. Table IV shows the positioning errors under various elevation mask angles. The cut-off elevation angles are tested in 5° and 10° as they are both popular. However, the elevation mask angle was set to 10° because it has the highest positioning accuracy. The 10° elevation angle is adjusted as a minimum angle. When the elevation angle of the satellite is lower than the angle, this satellite is excluded.

Table IV
Mean and Standard deviation statistics of positioning errors for L1/L2/E1 under different elevation mask angel.

Elevation mask angels	Positioning error	GPS L1	GPS L2	GAL E1
10°	Mean East (m)	1.6	3.4	0.3
	Mean North (m)	0.3	0.5	0.2
	Mean Up (m)	1.9	3.5	1.5
	Std. East (m)	1.5	5.4	0.7
	Std. North (m)	1.5	5.0	0.3
	Std. Up (m)	2.9	10.1	0.8
5°	Mean East (m)	1.8	3.6	0.1
	Mean North (m)	0.4	0.7	0.3
	Mean Up (m)	2.2	3.8	1.3
	Std. East (m)	1.2	4.3	0.7
	Std. North (m)	1.0	3.5	0.3
	Std. Up (m)	2.4	8.5	0.8

E. Troposphere Error Correction

The troposphere layer is made up of some gas components, these gases cause GNSS signals to refract which affects the GNSS signals' velocity, resulting in some propagation delay that affects the pseudo range measurement. Table V indicates the mean and standard deviation of positioning errors under the effect of enable/ disable troposphere correction by using tropospheric refraction correction model [12].

Table V
Mean and Standard deviation statistics of positioning errors for L1/L2/E1 under Tropospheric correction.

Tropospheric Correction	Positioning error	GPS L1	GPS L2	GAL E1
with Tropo correction	Mean East (m)	1.49	2.15	0.39
	Mean North (m)	0.2	0.43	0.19
	Mean Up (m)	1.9	2.46	1.4
	Std. East (m)	3.1	17.2	1.34
	Std. North (m)	3.35	5.4	0.6
	Std. Up (m)	3.1	18.5	1.6
without Tropo correction	Mean East (m)	8.2	4.4	0.5
	Mean North (m)	1.7	0.94	0.66
	Mean Up (m)	8.1	5.1	6.7
	Std. East (m)	3.1	17.216	1.34
	Std. North (m)	3.35	5.4	0.6
	Std. Up (m)	3.1	18.5	1.6

F. Ionosphere Error Correction

The propagation of GNSS signals through the ionosphere is one of the sources of GNSS error, as the presence of charges/ions has a delay impact on the signals. Table VI displays the mean and standard deviation of positioning errors when ionosphere correction is enabled or disabled.

Table VI

Mean and Standard deviation statistics of positioning errors for L1/L2/E1 under Ionosphere correction.

Ionoshperic Correction	Positioning error	GPS L1	GPS L2	GAL E1
with Iono correction	Mean East (m)	0.871	2.2	0.5
	Mean North (m)	1	0.1	0.36
	Mean Up (m)	1.026	2.85	0.32
	Std. East (m)	3.1	17.2	1.34
	Std. North (m)	3.35	5.4	0.6
	Std. Up (m)	3.1	18.5	1.6
without Iono correction	Mean East (m)	1.49	2.15	0.39
	Mean North (m)	0.2	0.43	0.19
	Mean Up (m)	1.9	2.46	1.4
	Std. East (m)	3.1	17.2	1.34
	Std. North (m)	3.35	5.4	0.6
	Std. Up (m)	3.1	18.5	1.6

G. Multi-GNSS Positioning Performance

This section compares the results of different signal combinations and demonstrated that a multi-GNSS position solution can help to improve accuracy. The tests were designed to ensure that the receiver provides a positioning solution that uses both Galileo and GPS. The positioning was done with the LSE method and the Precise Positioning (PP) technique. Table VII provides a statistical comparison of positioning results obtained using GPS or Galileo, or both GPS and Galileo under 4 different scenarios. This result is describing the mean and standard deviation for an output of 1700 position from each system using the optimized parameter mentioned above, Accordingly, the combination scenarios are presented.

Table VII

Comparison of positioning accuracy in meters using different combinations of navigation systems.

GNSS Signals	Mean East	Mean North	Mean Up	Std. East	Std. North	Std. Up
L1	0.8	0.9	1.04	3.06	3.31	3.12
L2	2	0.2	2.2	17.2	5.5	18.4
E1	0.47	0.33	0.43	2.95	1.4	1.6
L1+E1	0.304	0.404	0.095	1.6	0.7	1.9
L1+L2	0.195	0.134	0.858	4.1	4.58	5.574
L2+E1	0.769	0.392	0.515	5.531	2.614	6.3
L1+L2+E1	0.365	0.352	0.292	2.828	2.214	3.655

IV. CONCLUSIONS

The architecture and design of multi-GNSS software receiver is presented and optimized for GPS-L1, GPS-L2 and Galileo-E1. Experimental results were presented, where it was clearly demonstrated that using multi GNSS systems results in improved accuracy. According to the results, -shown Table VII- the combination of two or more GNSS signals results in enhancing the accuracy. For GPS signals, we can conclude that the four considered scenarios gave an optimized positioning solution compared to the single positioning solution, where the accuracy performance is improved by almost 50% by the combination. The GALILEO signal solution is optimized by roughly 10% when combined with GPS L1 and GPS L2 signals, while it's improved by nearly 16% when combined by GPS L1 only. However, it gives a negative effect on accuracy when combined with GPS L2 signal alone by almost 2%.

V. ACKNOWLEDGMENT

REFERENCES

[1] S. Söderholm, M. Z. H. Bhuiyan, and S. Thombre, "A multi-GNSS software-defined receiver : design , implementation , and performance benefits," Ann. Telecommun., pp. 399–410, 2016, doi: 10.1007/s12243-016-0518-7.

[2] H. Seok, D. Yoon, C. S. Lim, B. Park, S. W. Seo, and J. P. Park, "Study on GNSS Constellation Combination to Improve the Current and Future Multi-GNSS Navigation Performance," no. June 2015, 2016, doi: 10.11003/JPNT.2015.4.2.043.

[3] R. Acharya, Understanding Satellite Navigation. 2014.

[4] E. Kaplan and C. Hegarty, Understanding GPS. 2006.

[5] K. Borre, D. M. Akos, N. Bertelsen, P. Rinder, and S. H. Jensen, A Software-Defined GPS and Galileo Receiver A Single-Frequency Approach. 2004.

[6] J. B.-Y. Tsui, Fundamentals of Global Positioning System Receivers. 2005.

[7] E. Schönemann, "Analysis of GNSS raw observations in PPP solutions," 2013.

[8] A. Jovanovic, C. Mongrédien, Y. Tawk, C. Botteron, and P. A. Farine, "Two-step Galileo E1 CBOC tracking algorithm: When reliability and robustness are keys!," Int. J. Navig. Obs., vol. 2012, 2012, doi: 10.1155/2012/135401.

[9] O. Julien, "Design of Galileo L1F Receiver Tracking Loops UCGE Reports Number 20227 Department of Geomatics Engineering Design of Galileo L1F Receiver Tracking Loops," 2015.

[10] "Fraunhofer Flexiband," 2014.

[11] An Introduction to GNSS GPS, GLONASS, BeiDou, Galileo and other Global Navigation Satellite Systems Second Edition. 2010.

[12] E. D. Kaplan and C. J. Hegarty, Understanding GPS Principles and Applications Second Edition. 2006.

INTERNATIONAL JOURNAL
FOR RESEARCH

IN APPLIED SCIENCE & ENGINEERING TECHNOLOGY

Call : 08813907089   (24*7 Support on Whatsapp)